

A Joint Code and Belief Propagation Decoder Design for Quantum LDPC Codes

Sisi Miao, Jonathan Mandelbaum, Holger Jäkel, and Laurent Schmalen

Karlsruhe Institute of Technology (KIT), Communications Engineering Lab (CEL), 76187 Karlsruhe, Germany

Email: {firstname.lastname@kit.edu}

arXiv:2401.06874v1 [cs.IT] 12 Jan 2024

Abstract—Quantum low-density parity-check (QLDPC) codes are among the most promising candidates for future quantum error correction schemes. However, a limited number of short to moderate-length QLDPC codes have been designed and their decoding performance is sub-optimal with a quaternary belief propagation (BP) decoder due to unavoidable short cycles in their Tanner graphs. In this letter, we propose a novel joint code and decoder design for QLDPC codes. The constructed codes have a minimum distance of about the square root of the block length. In addition, it is, to the best of our knowledge, the first QLDPC code family where BP decoding is not impaired by short cycles of length 4. This is achieved by using an ensemble BP decoder mitigating the influence of assembled short cycles. We outline two code construction methods based on classical quasi-cyclic codes and finite geometry codes. Numerical results demonstrate outstanding decoding performance over depolarizing channels.

Index Terms—Quantum error correction, LDPC codes, belief propagation decoding

I. INTRODUCTION

Quantum low-density parity-checks (QLDPCs) codes are among the most promising candidates for future quantum error correction (QEC) schemes [1]. Various promising code constructions have been proposed, e.g., [2]–[6]. Still, some challenges remain. First, only a small number of good short to moderate-length QLDPC codes have been constructed, which are of special interest due to their low implementation complexity and their low decoding latency. Second, most construction methods ignore the structure of the underlying Tanner graph of the constructed codes. Thus, unavoidable short cycles of length 4 significantly impair the quaternary belief propagation (BP) decoding performance. However, the good decoding performance for classical LDPC codes and low decoding latency make BP an attractive candidate for QEC. Therefore, many previous works have tried to improve the decoding performance in the presence of short cycles, e.g., by modifying the BP decoder [7]–[10], or by introducing post-processing steps such as ordered statistics decoding (OSD) [9], [11]. However, these approaches cannot guarantee to completely mitigate the influence of the short cycles. Furthermore, the extra decoding latency introduced by these methods makes them less appealing for QEC where linear or even constant time decoding complexity is desired to achieve ultra-low

latency decoding. For example, the complexity of OSD is $\mathcal{O}(n^3)$ while the complexity of BP decoding is only $\mathcal{O}(n)$.

In this work, we construct short to moderate-length QLDPC codes with a good decoding performance with only BP decoding, achieved by joint code and decoder design such that the proposed ensemble BP decoding is not impaired by short cycles of length 4. The proposed scheme is referred to as **CAMEL** (Cycle Assembling and Mitigating with Ensemble decoding). We introduce two exemplary code construction methods in this paper. The first one is constructed from classical quasi-cyclic (QC) codes. The second one reuses the construction in [4] which is based on finite geometries (FGs). We evaluate the performance of CAMEL with numerical simulations over depolarizing channels.

Notation: Boldface letters denote vectors and matrices, e.g., \mathbf{a} and \mathbf{A} . The i -th component of vector \mathbf{a} is denoted by a_i , and the element at the i -th row and j -th column of \mathbf{A} is denoted by $A_{i,j}$. Let $\mathbf{A}_{i,:}$ be the i -th row of a matrix \mathbf{A} and $\mathbf{A}_{:,i}$ the i -th column of \mathbf{A} . \mathbf{A}^\top denotes the matrix transpose. The set $\{0, 1, 2, \dots, p-1\}$ is denoted by $[p]$ for any $p \in \mathbb{N}$. The trace inner product for $x, y \in \mathbb{F}_4$ is written as $\langle x, y \rangle \in \{0, 1\}$. It evaluates to 1 if $x \neq 0, y \neq 0$ and $x \neq y$, and 0 otherwise. We use \oplus to denote binary summation. The indicator function is denoted by $\mathbb{1}_{\{\cdot\}}$. Throughout the letter, the indexing of vector and matrix elements always starts from 0.

II. PRELIMINARIES

We consider a Calderbank–Shor–Steane (CSS) type quantum stabilizer code (QSC) [12] given by Theorem 1.

Theorem 1. Consider two classical binary linear codes \mathcal{C}_1 and \mathcal{C}_2 with parameters $[n, k_1, d_1]$ and $[n, k_2, d_2]$. Their parity check matrices (PCMs) are $\mathbf{H}_X \in \mathbb{F}_2^{(n-k_1) \times n}$ and $\mathbf{H}_Z \in \mathbb{F}_2^{(n-k_2) \times n}$, respectively. If $\mathcal{C}_2^\perp \subseteq \mathcal{C}_1$, i.e., satisfying the so-called twisted condition

$$\mathbf{H}_X \mathbf{H}_Z^\top = \mathbf{0}, \quad (1)$$

an $[[n, k_1 + k_2 - n, \min\{d_1, d_2\}]]$ QSC can be constructed.

Unless mentioned differently, we restrict ourselves to the case where $k_1 = k_2 =: k$. Thus, the check matrix of the QSC is written as

$$\mathbf{S} = \begin{pmatrix} \omega \mathbf{H}_X \\ \bar{\omega} \mathbf{H}_Z \end{pmatrix} \in \mathbb{F}_4^{2(n-k) \times n} \quad (2)$$

This work has received funding from the European Research Council (ERC) under the European Union’s Horizon 2020 research and innovation programme (grant agreement No. 101001899) and the German Federal Ministry of Education and Research (BMBF) within the project Open6GHub (grant agreement 16KISK010).

with ω and $\bar{\omega}$ being elements of the Galois field $\mathbb{F}_4 = \{0, 1, \omega, \bar{\omega}\}$. Furthermore, \mathbf{H}_X and \mathbf{H}_Z being sparse matrices results in a QLDPC code.

To estimate the error $e \in \mathbb{F}_4^n$ that occurred, the syndrome $z \in \mathbb{F}_2^{2(n-k)}$ is measured on the stabilizer generators. For simulation purpose, the syndrome z is computed as $z_j = \bigoplus_{i \in [n]} \langle e_i, S_{j,i} \rangle$ with $j \in [2(n-k)]$. In this work, we perform quaternary BP decoding [14] on the Tanner graph associated with the check matrix \mathbf{S} . A Tanner graph is a bipartite graph with two sets of vertices: the variable nodes (VNs) corresponding to the code symbols and the check nodes (CNs) corresponding to the checks and thus to rows of \mathbf{S} . A VN v_i is connected to a CN c_j if the corresponding entry $S_{j,i} \neq 0$.

Note that (1) requires an even number of overlapping ones between any row of \mathbf{H}_X and any row of \mathbf{H}_Z . Therefore, the Tanner graph associated with \mathbf{S} has a girth of either infinity or 4. First, if the Tanner graph has a girth of infinity, i.e., it is a tree, then the Tanner graphs associated with \mathbf{H}_X and \mathbf{H}_Z are necessarily trees. Such binary codes are known to have poor minimum distance [13]. Hence, short cycles are necessary in constructing good QLDPC codes. However, the Tanner graph structure needs careful optimization for BP decoding. One potential solution is to construct component matrices \mathbf{H}_X and \mathbf{H}_Z with a girth of at least 6 yet permitting 4-cycles between \mathbf{H}_X and \mathbf{H}_Z , as, e.g., done in [3]. Therefore, acceptable performance can be attained by decoding the \mathbf{X} and \mathbf{Z} errors separately using two binary BP decoders operating on the PCMs \mathbf{H}_Z and \mathbf{H}_X , respectively. However, binary decoding ignores the correlation between \mathbf{X} and \mathbf{Z} errors and is thus inherently sub-optimal, see, e.g., [7], [9], [10] for a performance comparison. Hence, to take the correlation into account while still mitigating the influence of short cycles, we propose CAMEL, a novel code construction where an ensemble of quaternary BP decoding is not impaired by short cycles of length 4.

III. CAMEL: JOINT CODE AND DECODER DESIGN

CAMEL consists of the construction of codes where all short cycles are assembled onto a single VN and an ensemble BP decoder in which the influence of short cycles is fully mitigated.

To this end, we first construct two classical binary LDPC codes whose parity check matrices $\mathbf{H}_1, \mathbf{H}_2 \in \mathbb{F}_2^{m \times n}$ fulfill

$$\mathbf{H}_1 \mathbf{H}_2^T = \mathbf{1}_{m \times m}, \quad (3)$$

where $\mathbf{1}_{m \times m}$ denotes an all-one matrix of size $m \times m$. It is possible to construct \mathbf{H}_1 and \mathbf{H}_2 fulfilling (3) such that the Tanner graph associated with the matrix $(\mathbf{H}_1^T \ \mathbf{H}_2^T)^T$ has a girth of at least 6. Two explicit code constructions will be presented in the following sections.

Next, we construct two new PCMs by appending an all-one column vector $\mathbf{1}_{m \times 1}$ to \mathbf{H}_1 and \mathbf{H}_2 , respectively, resulting in

$$\mathbf{H}_X = (\mathbf{H}_1 \mid \mathbf{1}_{m \times 1}) \in \mathbb{F}_2^{m \times (n+1)}$$

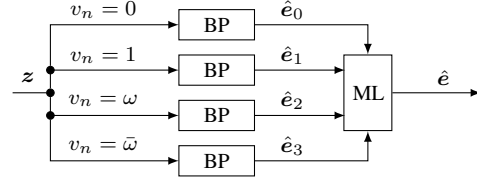


Figure 1. Block diagram of the proposed ensemble decoder.

and

$$\mathbf{H}_Z = (\mathbf{H}_2 \mid \mathbf{1}_{m \times 1}) \in \mathbb{F}_2^{m \times (n+1)}.$$

Then, we can verify that

$$\mathbf{H}_X \mathbf{H}_Z^T = (\mathbf{H}_1 \mid \mathbf{1}) \begin{pmatrix} \mathbf{H}_2^T \\ \mathbf{1}^T \end{pmatrix} = \mathbf{H}_1 \mathbf{H}_2^T + \mathbf{1}_{m \times m} = \mathbf{0}$$

and (1) is fulfilled. Note that all cycles of length 4 are nested on v_n . Then, using Theorem 1, we obtain an $[[n+1, n+1 - \text{rank}(\mathbf{H}_X) - \text{rank}(\mathbf{H}_Z), d]]$ QLDPC code.

We proceed by introducing the decoder part of CAMEL which essentially relies on ensemble decoding [16]. As depicted in Fig. 1, after measuring the syndrome z , four BP decodings are performed in parallel. In each BP decoding, the last bit is assigned a distinct fixed value $\eta \in \mathbb{F}_4$. The effect of doing so will be discussed below.

Let \hat{e}_i denote the error estimate of the BP decoding in the i -th path of the decoder shown in Fig. 1 and define $\mathcal{I} := \{i \in [4] : \hat{e}_i \text{ satisfies syndrome } z\}$. If $|\mathcal{I}| = 0$, the decoder declares a decoding failure. Otherwise, we perform a *maximum likelihood (ML)-in-the-list* step by choosing the error candidate $\hat{e} = \hat{e}_{i^*}$, $i^* \in \mathcal{I}$, of lowest weight, i.e., $i^* = \arg \min_{i \in \mathcal{I}} w(\hat{e}_i)$ where $w(\cdot)$ denotes the number of nonzero elements in the argument.

The approach of decoding using multiple decoders with hard guesses for certain bits is known as *decimation* in classical coding theory, e.g., in [17]. Next, we analyze the influence of decimating one bit in BP decoding for QLDPC codes. To this end, we consider a quaternary BP decoder passing probabilities. One can verify that the upcoming conclusions also hold for BP decoders with log-likelihood ratio (LLR) message passing [14], [15] and their refined version [7].

Assume that we provide the decoder with the hard guess η of the last VN, i.e., $v_n = \eta$. For an arbitrary decoding iteration, the outgoing message vector of v_n to a neighboring CN c_j is $(m_{v,n \rightarrow j}^{(0)} \ m_{v,n \rightarrow j}^{(1)} \ m_{v,n \rightarrow j}^{(\omega)} \ m_{v,n \rightarrow j}^{(\bar{\omega})})$ where

$$m_{v,n \rightarrow j}^{(a)} = b \cdot P_{\text{ch}}(v_n = a) \prod_{j' \in \mathcal{M}(n) \setminus \{j\}} m_{c,j' \rightarrow n}^{(a)} \quad (4)$$

for $a \in \mathbb{F}_4$ with $\mathcal{M}(i)$ denoting the set of indices of the neighboring CNs of VN v_i . The parameter b is a normalization factor such that the probabilities sum up to 1. As we provide a hard guess of $v_n = \eta$, the channel probability is $P_{\text{ch}}(v_n = a) = \mathbb{1}_{\{a=\eta\}}$. Therefore, the outgoing message of v_n in (4) evaluates to

$$m_{v,n \rightarrow j}^{(a)} = \mathbb{1}_{\{a=\eta\}}, \quad (5)$$

regardless of the incoming messages from the CNs. We now inspect the outgoing message of a CN c_j that is a neighbor of the decimated VN v_n , i.e., $j \in \mathcal{M}(n)$:

$$m_{c_j \rightarrow i}^{(a)} = c \cdot \sum_{t: t_i = a} f_{S_{j,:}}(t, z_j) \prod_{i' \in \mathcal{N}(j) \setminus \{i\}} m_{v_{i'} \rightarrow j}^{(t_{i'})} \quad (6)$$

where c is again some normalization factor and $\mathcal{N}(j)$ denotes the set of indices of the neighboring VNs of c_j . The check function $f_{S_{j,:}}(t, z_j)$ indicates if an error vector t fulfills the syndrome z_j specified by the j -th row of the check matrix $S_{j,:}$, i.e., $f_{S_{j,:}}(t, z_j) = 1$ if $\bigoplus_{i \in \mathcal{N}(j)} \langle t_i, S_{j,i} \rangle = z_j$ and 0 otherwise. Together with (5), we derive that for any $i \in \mathcal{N}(j), i \neq n$, the outgoing message in (6) is

$$\begin{aligned} m_{c_j \rightarrow i}^{(a)} &= c \cdot \sum_{t: t_i = a, t_n = \eta} f_{S_{j,:}}(t, z_j) \prod_{i' \in \mathcal{N}(j) \setminus \{i, n\}} m_{v_{i'} \rightarrow j}^{(t_{i'})} \\ &= c \cdot \sum_{t_{\sim n}: t_i = a} \langle \eta, S_{j,n} \rangle \oplus f_{S_{j,\sim n}}(t_{\sim n}, z_j) \prod_{i' \in \mathcal{N}(j) \setminus \{i, n\}} m_{v_{i'} \rightarrow j}^{(t_{i'})}, \quad (7) \end{aligned}$$

where $t_{\sim n}$ and $S_{j,\sim n}$ denote t and $S_{j,:}$ excluding their last entry, i.e., t_n and $S_{j,n}$, respectively.

From (7), it follows that messages associated with v_n are excluded in BP, except for $\langle \eta, S_{j,n} \rangle$, which is a constant. Thus, v_n can be removed together with all edges incident to it. This essentially dissolves all short cycles of length 4 in each decoding path as they are all assembled on v_n . Hence, their influence is fully mitigated.

IV. QUASI-CYCLIC QLDPC CODES

In [3], a class of QC QLDPC codes without short cycles of length 4 in their component matrices H_X and H_Z were constructed. In this section, we adapt this method to construct codes fulfilling (3). We first introduce a few definitions.

Let p be a prime number and \mathbb{F}_p be the prime field. We focus on a class of classical binary QC LDPC codes defined as the null space of a PCM

$$\mathbf{H} = \begin{pmatrix} I(c_{0,0}) & I(c_{0,1}) & \cdots & I(c_{0,L-1}) \\ I(c_{1,0}) & I(c_{1,1}) & \cdots & I(c_{1,L-1}) \\ \vdots & \vdots & \ddots & \vdots \\ I(c_{J-1,0}) & I(c_{J-1,1}) & \cdots & I(c_{J-1,L-1}) \end{pmatrix} \in \mathbb{F}_2^{Jp \times Lp}, \quad (8)$$

obtained by replacing each element $c_{i,j} \in [p]$ of a base matrix $\mathcal{H} \in [p]^{J \times L}$ by a circulant permutation matrix (CPM) $I(c_{i,j})$. A CPM $I(x)$ is obtained by cyclically right shifting all the rows of the identity matrix $\mathbf{I} \in \mathbb{F}_2^{p \times p}$ by x positions. For brevity, we denote the procedure of obtaining a binary PCM from a base matrix \mathcal{H} as $\mathbf{H} = \text{Cyc}(\mathcal{H})$. Note that the commutative group of CPMs $I(x)$ with $x \in [p]$ under matrix multiplication is isomorphic to the additive group of \mathbb{F}_p as $I(x)I(y) = I((x+y) \bmod p)$. Furthermore, for a commutative group \mathcal{G} and a subgroup \mathcal{G}' of \mathcal{G} , the coset of $g \in \mathcal{G}$ w.r.t. \mathcal{G}' is defined as $[g]_{\mathcal{G}'} := \{gh : h \in \mathcal{G}'\}$. Note that two cosets are either identical or disjoint.

Following the notation of [3], a vector $\mathbf{x} \in \mathbb{F}_p^L$ is called *multiplicity odd* if every element of \mathbf{x} occurs an odd number of times and *multiplicity free* if every element of \mathbf{x} is unique.

The vector \mathbf{x} is a *permutation vector* if it contains all elements of \mathbb{F}_p exactly once. Hence, a permutation vector of length p is multiplicity odd and free. Next, we need Lemma 1.

Lemma 1. Consider two matrices $\mathcal{A} \in \mathbb{F}_p^{J_1 \times L}$ and $\mathcal{B} \in \mathbb{F}_p^{J_2 \times L}$. Then, $\text{Cyc}(\mathcal{A})\text{Cyc}(\mathcal{B})^\top = \mathbf{1}_{J_1 p \times J_2 p}$ if and only if the difference vector between any two rows of \mathcal{A} and \mathcal{B} is multiplicity odd and contains all elements of \mathbb{F}_p .

Proof. Let \mathbf{a} be an arbitrary row of \mathcal{A} and \mathbf{b} be a row of \mathcal{B} . First, we have:

$$\text{Cyc}(\mathbf{a})\text{Cyc}(\mathbf{b})^\top = \sum_{i=0}^{L-1} I(a_i)I(b_i)^\top = \sum_{i=0}^{L-1} I(a_i - b_i).$$

This is a summation of L CPMs. Note that the ones in two CPMs either completely overlap or do not overlap at all. To ensure that $\sum_{i=0}^{L-1} I(a_i - b_i) = \mathbf{1}_{p \times p}$, the set $\{a_i - b_i : i \in [L]\}$ must contain all elements of \mathbb{F}_p an odd number of times. Thus, the difference vector of any two rows \mathbf{a} and \mathbf{b} must be multiplicity odd and contain all elements of \mathbb{F}_p at least once. As this holds for any two rows, it concludes the proof. \square

In order to obtain an all-one matrix, Lemma 1 implies $L \geq p$. Yet $L > p$ implies a Tanner graph with girth 4 [3]. Hence, we choose $L = p$. In this case, the set $\{a_i - b_i : i \in [L]\}$ yields a permutation vector and a check matrix with girth at least 6 can be constructed, as shown by Theorem 2.

Theorem 2. Let p be a prime number. There exists a base matrix $\mathcal{H} \in \mathbb{F}_p^{\ell \times p}$ with $\ell \leq p - 1$ such that any partition of \mathcal{H} into $\mathcal{H} = (\mathcal{H}_1^\top \quad \mathcal{H}_2^\top)^\top$ yields $\text{Cyc}(\mathcal{H}_1)\text{Cyc}(\mathcal{H}_2)^\top = \mathbf{1}$. Besides, the Tanner graph of $\text{Cyc}(\mathcal{H})$ has girth at least 6.

Proof. The proof is constructive. Let $\mathbb{F}_p^* := \mathbb{F}_p \setminus \{0\}$ denote the multiplicative group of \mathbb{F}_p . Additionally, let $\sigma \in \mathbb{F}_p^*$ be of order $\text{ord}(\sigma) = \ell$. Then, $\mathcal{G}' = \{\sigma^0, \dots, \sigma^{\ell-1}\}$ forms a subgroup of \mathbb{F}_p^* . We now form $T = |\mathbb{F}_p^*|/\ell$ cosets $[\tau_i]_{\mathcal{G}'}$ of size ℓ by choosing τ_i in the following way. First, let $\tau_0 = 1$. Then, for $i \in \{1, 2, \dots, T-1\}$, we consecutively choose $\tau_i \in \mathbb{F}_p^* \setminus \bigcup_{j=0}^{i-1} [\tau_j]_{\mathcal{G}'}$. This choice ensures that every τ_i belongs to a distinct coset. Now, form the matrix

$$\mathbf{M} = \begin{pmatrix} 1 & \sigma & \cdots & \sigma^{\ell-1} \\ \sigma^{\ell-1} & 1 & & \sigma^{\ell-2} \\ \vdots & & \ddots & \vdots \\ \sigma & \sigma^2 & \cdots & 1 \end{pmatrix} \in (\mathbb{F}_p^*)^{\ell \times \ell},$$

as well as the matrix

$$\mathcal{H} = (\mathbf{1}_{\ell \times 1} \quad \tau_0 \mathbf{M} \quad \cdots \quad \tau_{T-1} \mathbf{M}) \in (\mathbb{F}_p^*)^{\ell \times p}.$$

Let $\mathcal{H}_{j_1,:}$ and $\mathcal{H}_{j_2,:}$ be two distinct rows of \mathcal{H} , i.e., $j_1, j_2 \in [T], j_1 \neq j_2$. Their difference vector $\mathbf{d} := \mathcal{H}_{j_1,:} - \mathcal{H}_{j_2,:}$ can be written as $\mathbf{d} = (0 \quad \mathbf{d}^{(0)} \quad \mathbf{d}^{(1)} \quad \cdots \quad \mathbf{d}^{(T-1)}) \in \mathbb{F}_p^p$ where for $i \in [T]$,

$$\mathbf{d}^{(i)} = \tau_i \cdot (\mathbf{M}_{j_1} - \mathbf{M}_{j_2}) := \begin{pmatrix} d_0^{(i)} & d_1^{(i)} & \cdots & d_{\ell-1}^{(i)} \end{pmatrix} \in \mathbb{F}_p^\ell.$$

TABLE I
QC CODE CONSTRUCTED WITH $\text{ord}(\sigma)=p-1$.

Code	n	k	rate	p	σ	d
Q1	50	12	0.24	7	3	6
Q2	122	20	0.16	11	2	12
Q3	170	24	0.14	13	2	14
Q4	290	32	0.11	17	3	18
Q5	362	36	0.10	19	3	20

For $x \in [\ell]$, we write

$$d_x^{(i)} = \tau_i \cdot (\sigma^{\ell-j_1+x} - \sigma^{\ell-j_2+x}) = \tau_i \cdot (\sigma^{-j_1} - \sigma^{-j_2}) \cdot \sigma^{\ell+x}.$$

Thus, one can see that

$$\left\{ d_x^{(i)} : x \in [\ell] \right\} \equiv [\tau_i(\sigma^{-j_1} - \sigma^{-j_2})]_{\mathcal{G}'}$$

Therefore, the sets $\{d_x^{(i)} : x \in [\ell]\}$ for $i \in [T]$ yield the T distinct cosets permuting all elements in \mathbb{F}_p^* . Together with the first 0 element, \mathbf{d} forms a permutation vector of \mathbb{F}_p . Performing an arbitrary partition of \mathcal{H} into $\mathcal{H} = (\mathcal{H}_1^T \ \mathcal{H}_2^T)^T$ with $\mathcal{H}_1 \in (\mathbb{F}_p^*)^{\ell_1 \times p}$, $\mathcal{H}_2 \in (\mathbb{F}_p^*)^{\ell_2 \times p}$, and $\ell_1 + \ell_2 = \ell$ and using Lemma 1, we know that $\text{Cyc}(\mathcal{H}_1)\text{Cyc}(\mathcal{H}_2)^T = \mathbf{1}$. In this work, ℓ is always an even number and we choose $\ell_1 = \ell_2$.

It remains to show that the Tanner graph of $\text{Cyc}(\mathcal{H})$ has girth at least 6 which is fulfilled if the difference vector of any two rows of $\text{Cyc}(\mathcal{H})$ is multiplicity free [3]. This condition is met because the difference vectors of the rows of \mathcal{H} are permutation vectors. \square

We use the matrices \mathbf{H}_1 and \mathbf{H}_2 from the proof of Theorem 2 to construct QSCs as described in Sec. III. The parameters of the constructed codes are listed in Tab. I

Example. We consider an example for $p = 7$. Choosing $\sigma = 3$ yields the subgroup $\mathcal{G}' = [7]$. Note that $\text{ord}(\sigma) = 6$ and $T = 1$. Then, choose $\tau_0 = 1 \in [1]_{\mathcal{G}'}$. Since $T = 1$, no more τ_i are required. Hence, we can construct the base matrix

$$\mathcal{H} = (\mathbf{1}_{\ell \times 1} \ \tau_0 \mathbf{M}) = \begin{pmatrix} 1 & 1 & 3 & 2 & 6 & 4 & 5 \\ 1 & 5 & 1 & 3 & 2 & 6 & 4 \\ 1 & 4 & 5 & 1 & 3 & 2 & 6 \\ 1 & 6 & 4 & 5 & 1 & 3 & 2 \\ 1 & 2 & 6 & 4 & 5 & 1 & 3 \\ 1 & 3 & 2 & 6 & 4 & 5 & 1 \end{pmatrix}.$$

One can verify that the difference of any two rows, computed in \mathbb{F}_p , results in a permutation vector of \mathbb{F}_p . Note that we choose $T = 1$ as it yields low-rate codes, which are suitable for the current quantum channels with high noise level. We take the first three rows of \mathcal{H} to be \mathcal{H}_1 and the last three rows to be \mathcal{H}_2 . Then, we obtain two binary matrices $\text{Cyc}(\mathcal{H}_1)$ and $\text{Cyc}(\mathcal{H}_2) \in \mathbb{F}_2^{21 \times 49}$, both with rank 19.¹ By appending an all-one column to them, we obtain the Q1 code.

¹Note that \mathbf{H} is almost never of full rank. Therefore, the constructed codes naturally have an overcomplete set of stabilizers that will all be used for decoding. The same holds for the codes constructed in Sec. V. The benefits and complexity of this approach are discussed in [10].

V. QLDPC CODES FROM FINITE GEOMETRIES

In [4], a QLDPC code construction using FGs fulfilling (3) was proposed. We briefly review the construction and focus on concrete examples of the constructed codes and their decoding performance with CAMEL.

Consider a set \mathcal{N} of N points and a set \mathcal{M} of M lines constructed from a certain finite field. Details on the construction method can be found in [18], [19]. The points and lines form an FG if the following conditions are satisfied for some fixed integers $\gamma \geq 2$ and $\rho \geq 2$:

- (1) Each line passes through ρ points,
- (2) any two points are on exactly one line,
- (3) each point lies on γ lines,
- (4) two lines are either parallel or intersect at one and only one point.

In this work, we use the 2D-FGs based on finite fields \mathbb{F}_q of characteristic 2 with $q = 2^s$. This yields codes with the best minimum distances and decoding performance among the codes we constructed using FGs. Then, we focus on the most famous examples of FGs which are the Euclidean geometries (EGs) and the projective geometries (PGs). A 2D-EG consists of $N = q^2$ points and $M = q^2 + q$ lines. Moreover, we have $\rho = q$ and $\gamma = q + 1$. A 2D-PG contains $N = q^2 + q + 1$ points and $M = q^2 + q + 1$ lines where $\rho = q + 1$ and $\gamma = q + 1$.

We index the points in an FG from 0 to $N - 1$. For each line in an FG, indexed from 0 to $M - 1$, define an *incidence vector* $\mathbf{a} \in \mathbb{F}_2^N$ as follows: for $i \in [N]$, $a_i = 1$ if the point i is on the line and $a_i = 0$ otherwise.

Now, form a binary PCM $\mathbf{H} \in \mathbb{F}_2^{N \times M}$ whose columns consist of the incidence vectors of all lines in the FG. It follows that \mathbf{H} has a row weight of γ and a column weight of ρ . Moreover, it was shown in [19] that the minimum distance of the binary linear code defined by \mathbf{H} is lower bounded by ρ .

For this binary PCM $\mathbf{H} \in \mathbb{F}_2^{N \times M}$, it is easy to show that $\mathbf{H}\mathbf{H}^T = \mathbf{1}$ using condition (2) and with our assumption that $q = 2^s$.² To construct QLDPC codes with relatively low rates, we choose $\mathbf{H}_X = \mathbf{H}_Z = (\mathbf{H} \mid \mathbf{1}) \in \mathbb{F}_2^{N \times (M+1)}$.³ One can verify that the minimum distance of the code defined by the PCM $(\mathbf{H} \mid \mathbf{1})$ is the same as the minimum distance of the code defined by \mathbf{H} , which is lower bounded by ρ . Therefore, for codes constructed from the 2D-FG, the minimum distance is approximately \sqrt{n} .

The parameters of the exemplary codes constructed from EGs are listed in Tab. II. As for the PG codes, assume that a QLDPC code constructed from an EG using a finite field has parameters $[[n, k, d]]$. Then, the QLDPC code constructed from

²We have to point out a mistake in [4] where the columns of \mathbf{H} are the incidence vectors of the lines which *do not pass through origin* instead of *all the lines* in the geometry as we do. We can verify that the former does not yield a matrix \mathbf{H} that fulfills (3) by looking at any two non-origin points i and j located on a line λ which passes through the origin. In our construction, it means that the λ -th column is the only column where the two rows $\mathbf{H}_{i,\cdot}$ and $\mathbf{H}_{j,\cdot}$ have an overlapping one as two points are on exactly one line. Therefore, $\mathbf{H}_{i,\cdot}\mathbf{H}_{j,\cdot}^T = 1$. Thus, removing column $\mathbf{H}_{\cdot,\lambda}$ leads to $\mathbf{H}_{i,\cdot}\mathbf{H}_{j,\cdot}^T = 0$.

³This unfortunately introduces some short cycles of length 4 between \mathbf{H}_X and \mathbf{H}_Z . However, thanks to the other good properties of the FG codes, the performance degradation is acceptable.

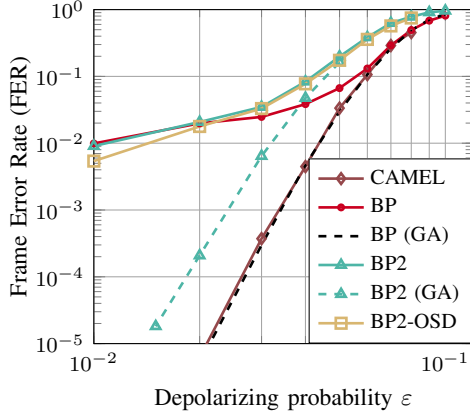


Figure 2. FER vs. depolarizing probability ε curves when decoding an E4 $[[273, 111, 17]]$ QLDPC code from an EG using different decoding algorithms.

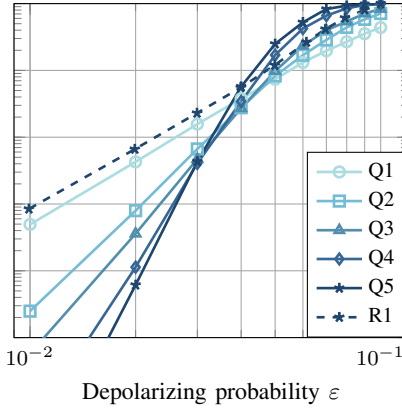


Figure 3. FER vs. depolarizing probability ε curves for the quasi-cyclic QLDPC codes shown in Tab. I and the reference code R1.

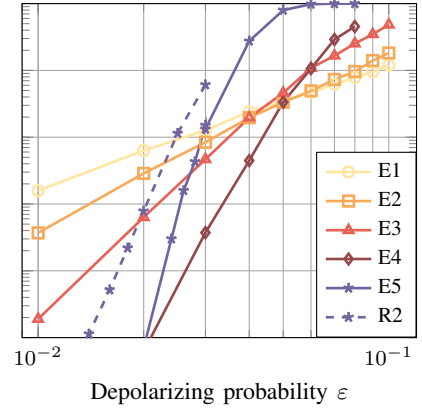


Figure 4. FER vs. depolarizing probability ε curves for QLDPC codes constructed using EGs shown in Tab. II and the reference code R2.

TABLE II
QLDPC CODES FROM 2D EG OF FINITE FIELD OF CHARACTERISTIC 2.

Code	n	k	rate	s	d
E1	7	1	0.14	1	3
E2	21	3	0.14	2	5
E3	73	19	0.26	3	9
E4	273	111	0.41	4	17
E5	1057	571	0.54	5	33

a PG using the same field has parameters $[[n+1, k+1, d+1]]$. Hence, we do not list them explicitly.

VI. NUMERICAL RESULTS

We assess the proposed scheme using Monte Carlo simulations over the quantum depolarizing channel where the three types of Pauli errors occur with equal probability $\varepsilon/3$. At least 300 frame errors are collected to obtain the frame error rate (FER) for each data point. All BP decoding paths use sum-product algorithm with 15 iterations and a flooding schedule.

First, we highlight the importance of decoding using our proposed ensemble decoder. Figure 2 depicts the decoding results using different decoding algorithms for the E4 code as an example. When decoded with a single BP decoder, the decoding performance is poor due to numerous short cycles of length 4. However, when using ensemble decoding in CAMEL as described in Sec. III, the performance improves by orders of magnitude. Moreover, we evaluate a genie-aided (GA) BP decoder which is fed the correct value of v_n . The ensemble BP decoding has almost the same performance as the genie-aided version. As the reliability of the guessed value is set to infinity, corresponding to a probability of 1, the paths with the wrong guess usually either fail to converge or will find a high-weight error estimate. For completeness, we also plot the decoding results using a pair of binary BP (BP2) decoders and its genie-aided version where the correct value of v_n is fed to both decoders. They are outperformed by their respective quaternary counterpart. Furthermore, we decode the

E4 code using the BP2-OSD decoder implemented in [11]. However, the decoding gain achieved by the BP-OSD decoder is limited compared to the genie-aided BP2 decoder. For other constructed codes, we observe similar results.

We also compare the performance of the QLDPC codes constructed in Sec. IV and Sec. V using the proposed ensemble BP decoder with existing codes as depicted in Fig. 3 and Fig. 4, respectively. Our Q5 code outperforms the $[[400, 16]]$ hypergraph product code (R1) with BP-OSD decoder [11] and our E5 code outperforms the $[[800, 400]]$ bicycle code (R2) using the modified non-binary decoder with enhanced feedback [8], [20]. Note that both reference codes use a significantly more complex decoding algorithm and have lower code rates than our constructed codes. We conclude that CAMEL achieves great decoding performance with low-decoding latency.

VII. CONCLUSION

In this paper, we proposed a novel joint code and decoder design for QLDPC codes with good quaternary BP decoding performance without the need for any major modification of the BP decoder or any post-processing steps. Simulation results show a significant improvement compared to conventional BP decoding.

REFERENCES

- [1] D. Gottesman, "Fault-tolerant quantum computation with constant overhead," *Quantum Information and Computation*, vol. 14, 2014.
- [2] D. J. MacKay, G. Mitchison, and P. L. McFadden, "Sparse-graph codes for quantum error correction," *IEEE Trans. Inf. Theory*, vol. 50, no. 10, 2004.
- [3] M. Hagiwara and H. Imai, "Quantum quasi-cyclic LDPC codes," in *Proc. ISIT*, 2007.
- [4] S. A. Aly, "A class of quantum LDPC codes constructed from finite geometries," in *Proc. GLOBECOM*, 2008.
- [5] J.-P. Tillich and G. Zémor, "Quantum LDPC codes with positive rate and minimum distance proportional to the square root of the blocklength," *IEEE Trans. Inf. Theory*, vol. 60, no. 2, 2013.
- [6] P. Panteleev and G. Kalachev, "Asymptotically good quantum and locally testable classical LDPC codes," in *Proc. SIGACT Symposium on Theory of Computing*, 2022.

- [7] C.-Y. Lai and K.-Y. Kuo, "Log-domain decoding of quantum LDPC codes over binary finite fields," *IEEE Trans. Quantum Eng.*, vol. 2, 2021.
- [8] Z. Babar, P. Botsinis, D. Alanis, S. X. Ng, and L. Hanzo, "Fifteen years of quantum LDPC coding and improved decoding strategies" *IEEE Access*, vol. 3, 2015.
- [9] P. Panteleev and G. Kalachev, "Degenerate quantum LDPC codes with good finite length performance," *Quantum*, vol. 5, 2021.
- [10] S. Miao, A. Schnerring, H. Li, and L. Schmalen, "Quaternary neural belief propagation decoding of quantum LDPC codes with overcomplete check matrices," *arXiv preprint arXiv:2308.08208*, 2023.
- [11] J. Roffe, D. R. White, S. Burton, and E. Campbell, "Decoding across the quantum low-density parity-check code landscape," *Physical Review Research*, vol. 2, no. 4, 2020.
- [12] A. R. Calderbank, E. M. Rains, P. W. Shor, and N. J. A. Sloane, "Quantum error correction via codes over $GF(4)$," *IEEE Trans. Inf. Theory*, vol. 44, no. 4, 1998.
- [13] T. Etzion, A. Trachtenberg and A. Vardy, "Which codes have cycle-free Tanner graphs?," *IEEE Trans. Inf. Theory*, vol. 45, no. 6, 1999.
- [14] M. C. Davey and D. J. MacKay, "Low density parity check codes over $GF(q)$," in *Proc. ITW*, 1998.
- [15] D. Declercq and M. Fossorier, "Decoding algorithms for nonbinary LDPC codes over $GF(q)$," *IEEE Trans. Commun.*, vol. 55, no. 4, 2007.
- [16] T. Hehn, J. B. Huber, S. Laendner, and O. Milenkovic, "Multiple-bases belief-propagation for decoding of short block codes," in *Proc. ISIT*, 2007.
- [17] V. Aref, N. Macris, and M. Vuffray, "Approaching the rate-distortion limit with spatial coupling, belief propagation, and decimation," *IEEE Trans. Inf. Theory*, vol. 61, no. 7, 2015.
- [18] S. Lin and D. J. Costello, Jr., *Error Control Coding: Fundamentals and Applications*. Prentice-Hall, 2004.
- [19] Y. Kou, S. Lin, and M. Fossorier, "Low-density parity-check codes based on finite geometries: a rediscovery and new results," *IEEE Trans. Inf. Theory*, vol. 47, no. 7, 2001.
- [20] Y.-J. Wang, B. C. Sanders, B.-M. Bai, and X.-M. Wang, "Enhanced Feedback Iterative Decoding of Sparse Quantum Codes," *IEEE Trans. Inf. Theory*, vol. 58, no. 2, 2012.